

# Semiconductor Electrodes. 12. Photoassisted Oxidations and Photoelectrosynthesis at Polycrystalline TiO<sub>2</sub> Electrodes

Steven N. Frank and Allen J. Bard\*

Contribution from the Department of Chemistry, The University of Texas, Austin, Texas 78712. Received December 22, 1976

**Abstract:** The photoassisted oxidations of a number of compounds, including hydroquinone, *p*-aminophenol, I<sup>-</sup>, Br<sup>-</sup>, Cl<sup>-</sup>, Fe<sup>2+</sup>, Ce<sup>3+</sup>, and CN<sup>-</sup>, at polycrystalline TiO<sub>2</sub> are demonstrated. Many of these compounds compete for photogenerated holes with the solvent with high current efficiencies. Ethanol, CN<sup>-</sup>, and ethyl formate are oxidized by a current doubling mechanism. The majority of these compounds can be oxidized at the illuminated TiO<sub>2</sub> at potentials negative of their standard potentials. The compounds which are oxidized with high current efficiencies have markedly different current-potential curves than those obtained for the solvent alone. Possible synthetic applications and mechanisms for the competitive oxidations are discussed.

There has been much recent interest in the application of semiconductor electrodes, such as TiO<sub>2</sub>, to the photolysis of water and in systems for the direct conversion of solar to electrical energy.<sup>1-17</sup> In most of the previous studies with TiO<sub>2</sub> electrodes the process occurring at the electrode surface is the reaction of photogenerated holes with water to produce oxygen. However, studies of the oxidation of other solution species at semiconductor electrodes are also of interest for possible synthetic purposes and because such studies can provide information about the mechanism of such photoassisted processes. In synthetic applications photoassisted oxidations at n-type semiconductors (or reductions at p-type materials) can be carried out to produce new materials with light, rather than electrical or chemical energy, supplying the driving force for the reaction; this process can be called *photoelectrosynthesis*. Photochemical electron transfer reactions in homogeneous solutions are usually inefficient, because the electron transfer between the excited state and substrate produce oxidized and reduced species in close proximity and the back electron transfer reaction is thermodynamically favored. At a semiconductor electrode the band bending in the space charge region causes electron-hole pair separation; in an n-type material the electrons are carried away through the external circuit and the holes react at the surface. Moreover the use of the semiconductor electrode allows the photochemical reaction to be carried out at wavelengths characteristic of the semiconductor band gap rather than those needed to excite the substrate. For example, the oxidation of bromide ion in solution<sup>18</sup> requires much shorter wavelengths than are needed with even a wide band gap semiconductor. The same is true of the photoassisted oxidation of water.

The theory of the semiconductor/solution interface is discussed elsewhere<sup>19</sup> and in earlier papers of this series.<sup>20,21</sup> Illumination of a semiconductor electrode with light of energies greater than the band gap creates electron-hole pairs near the electrode/solution interface. For an n-type semiconductor such as TiO<sub>2</sub>, polarization of the electrode to potentials positive of the flat band potential (analogous to the zero charge potential for metals) results in electron-hole separation with holes forced to the surface. At the surface the holes may either participate in decomposition of the semiconductor lattice or be transferred to solution species. When transfer to solution occurs, substances other than the solvent may participate but the reactivity of holes with these must be much greater than those of the solvent to comprise a significant portion of the hole current. The actual reaction sequence can be quite complicated, e.g., for ZnO, lattice decomposition, solvent reactions,<sup>22,23</sup> and participation of other solution species all occur.<sup>24</sup> For elec-

trochemical solar devices long term electrode stability is necessary. Unfortunately, for most semiconductors with band gaps small enough to use a significant portion of the solar spectrum (e.g., Si, GaAs, GaP, InP, CdS), the predominant reaction under illumination is the dissolution or oxidation of the electrode surface<sup>25</sup> with a resulting degradation in electrode response. There is much interest in the suppression of such lattice decomposition reactions by introduction of solution species which can be oxidized at a much higher rate (e.g., the use of the sulfide-polysulfide system with CdS electrodes).<sup>13,14,23,24,26,27</sup> However, the factors governing how the photocurrent is apportioned among the various possible processes are still not well-understood. Although TiO<sub>2</sub> has a large band gap (ca. 3 eV) and thus makes inefficient use of solar energy, it has a number of advantages that make it useful for studying competitive oxidation reactions. Among these are the chemical and photochemical stability of TiO<sub>2</sub> over a wide range of solution conditions and the ease with which polycrystalline TiO<sub>2</sub> electrodes can be fabricated.<sup>4</sup> The present investigation concerns the photoassisted oxidation of solution components other than water at n-type TiO<sub>2</sub> polycrystalline electrodes with the intent of demonstrating the possible synthetic applicability of semiconductor electrodes and studying possible couples that react with the needed high current efficiencies suitable for electrochemical solar cells. We describe the photoassisted oxidation of a number of organic and inorganic compounds at TiO<sub>2</sub> carried out either under potentiostatic conditions at potentials negative of where their oxidations occur at platinum or in the absence of an external power supply with all of the energy for the transformation being supplied by light in a solar cell arrangement.

## Experimental Section

Most compounds used in this study were reagent grade quality and used without further purification except as noted. Aniline as received was contaminated with highly colored air oxidation products and was distilled from Zn dust collecting the fraction between 183 and 184 °C. Practical grade *p*-aminophenol (PAP), which was also contaminated with oxidation products, was purified as described in the literature.<sup>28</sup> It was used before significant oxidative darkening occurred.

All solutions were prepared with low conductivity water which showed no adsorption waves or electroactive impurities at platinum or mercury electrodes in solutions containing only electrolyte upon voltammetric investigation.

The polycrystalline TiO<sub>2</sub> electrodes were prepared by chemical vapor deposition onto titanium substrates.<sup>4</sup> The conductivity of the electrodes thus prepared was increased by heating at 650 °C under vacuum for 1 h. Contact to the titanium substrate was made with silver epoxy. The backs of the electrode were coated with Devcon 5 min

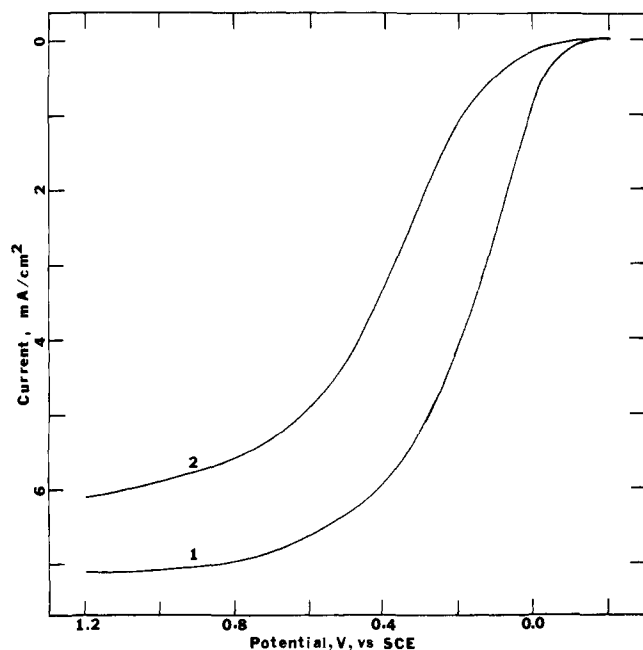


**Figure 1.** Current-potential curves for polycrystalline (1) and single-crystal (2)  $\text{TiO}_2$  during illumination with a 450 W Xenon lamp in 0.2 M  $\text{H}_2\text{SO}_4$ .

epoxy. The electrodes were mounted to hollow glass tubes with silicone cement (Dow-Corning) and all surfaces that were not  $\text{TiO}_2$  were coated with the silicone. The area of all of the polycrystalline  $\text{TiO}_2$  electrodes in this study was  $1.2 \pm 0.2 \text{ cm}^2$ . The  $\text{TiO}_2$  films were not exposed to a HF etching solution as in a previous study<sup>20</sup> because the HF caused flaking of the film at any defects. Instead, the electrodes were cleaned by exposing them for 30 s to concentrated  $\text{HNO}_3$ . This was sometimes supplemented by polishing the electrodes with  $0.5 \mu\text{m}$  alumina. The silicone cement was highly resistant to nitric acid but tended to incorporate some of the insoluble polymeric products in some experiments. No other complications were observed from using the silicone cement. Several experiments were repeated using a single crystal  $\text{TiO}_2$  electrode. The preparation of this electrode was described elsewhere.<sup>20</sup> The effective resistance of the electrode was decreased by electrochemically plating indium to the entire backside of the crystal.

The design of the electrochemical cell was similar to one used in an earlier study.<sup>20</sup> The cell was equipped with a side arm that permitted passing nitrogen both through and over the solution. The  $\text{TiO}_2$  electrode was either illuminated with the auxiliary and reference electrodes between the optical window and the  $\text{TiO}_2$  or with the  $\text{TiO}_2$  close to the optical window (0.5–1 cm) and the other electrodes positioned behind the  $\text{TiO}_2$ . Although the second arrangement represents rather poor cell geometry, there was very little difference in the current-potential curves between the two cell arrangements when positive feedback resistance compensation (adjusted to a point just short of potentiostat oscillation) was used. Because many of the compounds gave products that filtered UV radiation with a resulting decrease in current density, the second cell arrangement was the one used most often.

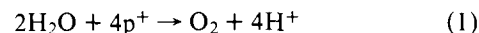
A small platinum disk ( $\sim 0.75 \text{ mm}^2$ ) sealed in glass was sometimes employed as a working electrode for monitoring changes in electrochemical behavior following illumination of the cell. The auxiliary electrode was a platinum foil and the reference electrode was a saturated calomel electrode (SCE).

A PAR Model 173 potentiostat with a Model 179 digital coulometer and current follower and a PAR Model 175 universal programmer (Princeton Applied Research Corp., Princeton, N.J.) were used for electrochemical experiments. Current-potential curves were recorded on a Houston Instruments Model 2000 X-Y recorder. In most experiments the cells were illuminated with an Oriel Model 6242 450 W Xenon lamp and power supply (Oriel Corporation of America, Stamford, Conn.). UV spectra were obtained with a Cary 14 spectrophotometer.

All solutions were deaerated with prepurified nitrogen before each experiment.

## Results

**$n\text{-TiO}_2$  in Supporting Electrolyte Solution.** A number of studies have dealt with the photoprocess which occurs at single crystal and polycrystalline  $\text{TiO}_2$  in the absence of readily oxidizable substances.<sup>1,7,8</sup> Briefly, at potentials positive of the flat-band potential ( $V_{fb}$ ) the oxidation of water by photogenerated holes ( $p^+$ ) occurs, as shown in eq 1.



The actual mechanism of this reaction is not known, and  $\text{H}_2\text{O}_2$  has also been detected in small quantities as a reaction product or intermediate.<sup>7</sup> Since this reaction occurs as the competitive background reaction in all of the experiments reported here, a brief description of the results with the  $\text{TiO}_2$  electrodes used in this study in supporting electrolyte is included. Typical  $i$ - $E$  curves for single crystal and polycrystalline (CVD)  $\text{TiO}_2$  under illumination are shown in Figure 1. Oxygen evolution occurs at potentials just positive of  $V_{fb}$ , which depends upon the solution pH<sup>29</sup> and which is nearly 0.9 V negative of the thermodynamic potential for oxygen evolution.<sup>30</sup> In the absence of illumination no anodic current is observed until potentials are sufficiently positive to allow tunneling and breakdown phenomena to occur.<sup>4,31,32</sup> With polycrystalline electrodes appreciable dark anodic currents begin to flow at +2 to +3 V vs. SCE.

The maximum quantum efficiency for irradiation with monochromatic light of energy greater than  $E_g$  and for electrode potentials on the current plateau region, which is defined as the current flow at the electrode (in electrons/s) divided by the light flux (in photons/s), is about 0.7 to 0.8 for single crystal materials and slightly lower for polycrystalline materials. These values are near those reported previously under similar conditions.<sup>33</sup> The quantum efficiency for the polycrystalline electrode in Figure 1 is about 0.6. However, the current density at the plateau, the general shape of the photocurrent- $E$  curve, and the efficiency are very dependent upon the method of preparation of the polycrystalline film and are apparently functions of film thickness and the extent of conversion of the  $\text{TiO}_2$  to the rutile crystal structure. We had no difficulty in obtaining electrodes with characteristics equal or superior to the one used for Figure 1. There was some decrease in the response of the polycrystalline electrodes after repeated polishing and following any inadvertent strong cathodic polarization where the resulting vigorous  $\text{H}_2$  evolution produces physical deterioration of the films. Otherwise, the electrodes were quite stable with time and after repeated usage.

**Current Efficiencies of Photosensitized Oxidations at  $n\text{-TiO}_2$ .** When oxidizable substances are added to the supporting electrolyte solution, the total anodic photocurrent will consist of contributions from the oxidation of these substance and the oxidation of water. The success with which a given compound competes with water for the photogenerated holes is expressed as the current efficiency, which is the fraction of the total current which results in the oxidation of the substance of interest. The integral current efficiencies for a number of substances, measured by determining either the amount of product formed or amount of reactant oxidized and dividing by the total number of coulombs passed during the photoelectrolysis at a given potential, are given in Table I. These current efficiencies are the maximum ones obtained at a given additive concentration and were determined by adjusting the illumination intensity with neutral density filters until the current efficiency was independent of intensity. The maximum current density for substrate oxidation is determined by the rate of mass transfer of substrate to the electrode surface. The total photocurrent is determined by the light intensity. Thus at high intensities the current efficiency for substrate oxidation will

**Table I.**<sup>a</sup> Current Efficiencies for the Photoassisted Electrooxidations of Various Compounds at TiO<sub>2</sub>

Compd	Concn, mM	Current efficiency	Electrolyte	E° redox V vs. SCE	V <sub>fb</sub> <sup>b</sup> V vs. SCE
I <sup>-</sup>	10	0.6 <sup>c</sup>	0.2 M H <sub>2</sub> SO <sub>4</sub>		-0.2
	10	0.6 <sup>d,e</sup>	0.2 M Na <sub>2</sub> SO <sub>4</sub>	0.29 <sup>f</sup>	-0.6
	100	0.8	0.2 M Na <sub>2</sub> SO <sub>4</sub>		-0.6
Br <sup>-</sup>	10	0.2 <sup>e</sup>	0.2 M Na <sub>2</sub> SO <sub>4</sub> + 5 mM H <sub>2</sub> SO <sub>4</sub>	0.82 <sup>f</sup>	-0.4
	100	0.3			
	1000	0.6			
Cl <sup>-</sup>	100	0.2 <sup>e</sup>	0.2 M Na <sub>2</sub> SO <sub>4</sub> + 5 mM H <sub>2</sub> SO <sub>4</sub>	1.1 <sup>f</sup>	-0.4
	1000	0.4			
Ce <sup>3+</sup>	10	0.1 <sup>g</sup>			
	30	0.4			
	100	0.7	0.2 M H <sub>2</sub> SO <sub>4</sub>	~1.2 <sup>f</sup>	-0.2
Fe <sup>2+</sup>	1000	0.7			
	10	0.4 <sup>g</sup>	0.2 M H <sub>2</sub> SO <sub>4</sub>	0.53 <sup>f</sup>	-0.2
	30	0.5			
Fe(CN) <sub>6</sub> <sup>4-</sup>	10	≈ Hydroquinone <sup>h</sup>	0.2 M H <sub>2</sub> SO <sub>4</sub>	0.12 <sup>f</sup>	-0.2
Hydroquinone	10	0.8 <sup>c</sup>	0.2 M H <sub>2</sub> SO <sub>4</sub>	0.46 <sup>f</sup>	-0.2
<i>p</i> -Aminophenol	10	0.6 <sup>c</sup>	0.2 M H <sub>2</sub> SO <sub>4</sub>	0.47 <sup>i</sup>	-0.2
Aniline	<1	Probably high <sup>j</sup>	0.2 M Na <sub>2</sub> SO <sub>4</sub> + 5 mM H <sub>2</sub> SO <sub>4</sub>	~0.9 <sup>h</sup>	-0.4
<i>N,N</i> -Dimethylaniline	<10	Probably high <sup>j</sup>	0.2 M H <sub>2</sub> SO <sub>4</sub>	>0.9 <sup>k</sup>	-0.2
CN <sup>-</sup>	1000	0.4 <sup>l</sup>	0.1 M NaOH	-1.2 <sup>f</sup>	-0.9
S <sup>2-</sup>	>1000	0 <sup>l</sup>	0.1 M NaOH	-0.26 <sup>f,m</sup>	-0.9
Ethanol	1000	0.1 <sup>l</sup>	0.1 M NaOH	~0.4 <sup>f</sup>	-0.9
Ethyl formate	1000	0.3 <sup>l</sup>	0.1 M NaOH		-0.9
	1000	0.2	0.1 M H <sub>2</sub> SO <sub>4</sub>		-0.2

<sup>a</sup> The electrochemical processes assumed for compounds 1-6, 9, and 10 are one-electron oxidations. The possible oxidation products for 9 and 10 are given by Adams, McClure, and Morris, *Anal. Chem.*, **30**, 471 (1958), and Bacon and Adams, *J. Am. Chem. Soc.*, **90**, 6596 (1968). Two-electron processes are assumed for compounds 7 and 8 and 11-14. The product of the two-electron oxidation of CN<sup>-</sup> is believed to be NCO<sup>-</sup>. <sup>b</sup> From ref 4 assuming the onset of the photocurrent for the electrolyte solution only corresponds to V<sub>fb</sub>. <sup>c</sup> Determined by oxidizing the remaining reactant at a platinum foil electrode. <sup>d</sup> Determined by titrating the thiosulfate, S<sub>2</sub>O<sub>3</sub><sup>2-</sup>, that remained after reaction with photogenerated product with standard I<sub>2</sub> to the starch end point. S<sub>2</sub>O<sub>3</sub><sup>2-</sup> was not oxidized at the TiO<sub>2</sub> at the concentrations employed, ~1 mM. <sup>e</sup> Determined by titrating the As(III) that remained after reaction with photogenerated product with standard I<sub>2</sub> to the starch end point. The pH was adjusted with acetate to increase the reaction rate. As(III) was not oxidized at the TiO<sub>2</sub> for concentrations ≤ 2 mM. <sup>f</sup> Value from ref 30. <sup>g</sup> Determined by reducing the photogenerated product at a platinum foil electrode. <sup>h</sup> Estimated by comparing the reductive peak heights at the TiO<sub>2</sub> of the photogenerated products. Products generated for 1 s at equal initial currents and the potential sweep into the reductive potential region. <sup>i</sup> From this work. <sup>j</sup> Products formed soluble polymeric films on the electrodes. These films formed even in the presence of >10 mM l<sup>-</sup>. <sup>k</sup> Not reversible thermodynamic values, because the initial product of oxidation is not stable (Adams, McClure, and Morris, *Anal. Chem.*, **30**, 471 (1958), and Bacon and Adams, *J. Am. Chem. Soc.*, **90**, 6596 (1968)). <sup>l</sup> Calculated by assuming the only oxidation path is one that leads to current doubling. <sup>m</sup> This value is about the same for a number of the possible polysulfide intermediates.

be mass transfer controlled and will be smaller than that at lower intensities. Under the conditions of the experiments in Table I the current efficiency does not depend upon the rate of mass transfer of the compound to the electrode surface. The current densities obtained depended upon the concentration of added compound and were as high as 3 mA/cm<sup>2</sup>. Throughout the experiment nitrogen was bubbled through the cell to scrub the solution of any oxygen produced at the TiO<sub>2</sub>. For most of the compounds control experiments at open circuit demonstrated that no significant spontaneous oxidation of the compounds would occur under illumination, even if oxygen were present. Iodide was an exception, however. The total coulombs passed, which is equivalent to the total number of holes transferred to solution, was determined by integrating the current. Usually, the amount of compound that reacted was determined either by a controlled potential oxidation of the remaining reactant or by measuring the amount of product formed, the latter being the preferred procedure. For Ce<sup>3+</sup> and Fe<sup>2+</sup> this was accomplished by a controlled potential coulometric reduction of the oxidation product. Because Fe(CN)<sub>6</sub><sup>4-</sup> and Fe(CN)<sub>6</sub><sup>3-</sup> are not stable when illuminated by UV radiation, voltammetric analysis, as described in the notes to Table I, was used to determine the current efficiency of ferrocyanide oxidation. The volatility of the products of I<sup>-</sup>, Br<sup>-</sup>, and Cl<sup>-</sup> oxidation precluded using direct product analysis. In this case the products were scavenged by S<sub>2</sub>O<sub>3</sub><sup>2-</sup> or As(III) as they were formed and the amount of S<sub>2</sub>O<sub>3</sub><sup>2-</sup> or As(III) that reacted was determined by titration with iodine.<sup>34,35</sup> At

the current densities and concentration employed, neither S<sub>2</sub>O<sub>3</sub><sup>2-</sup> nor As(III) were oxidized at the TiO<sub>2</sub> electrode as determined in control experiments. The oxidation products of hydroquinone (HQ) and *p*-aminophenol (PAP) apparently undergo further homogeneous photochemical reactions to produce new products with electrochemical behavior different from the quinones. For these the current efficiency was determined by measuring the unreacted HQ or PAP by coulometry. Control experiments at platinum showed that these follow up reactions have no effect on the current efficiency determined in this fashion.

Formation of insoluble polymeric films on the electrodes prevented finding the current efficiencies for aniline and *N,N*-dimethylaniline. Filming was apparent with less than 1 mM concentration of aniline and a 10 mM concentration of *N,N*-dimethylaniline even in the presence of iodide so that the current efficiencies for their oxidation must be high. Cyanide, sulfide, ethanol, and ethyl formate are substances which are known to produce "current doubling" at other semiconductor electrodes.<sup>24,36</sup> Current doubling involves the initial transfer of one electron to a photogenerated hole which results in the formation of an intermediate which is much more easily oxidized than the parent molecule and which can transfer a second electron to the semiconductor conduction band. Thus the photosensitized oxidation of such compounds results in currents twice as large as the intensity-limited saturation photocurrents of the one-electron substances. The current efficiencies for these compounds were calculated from the difference in the

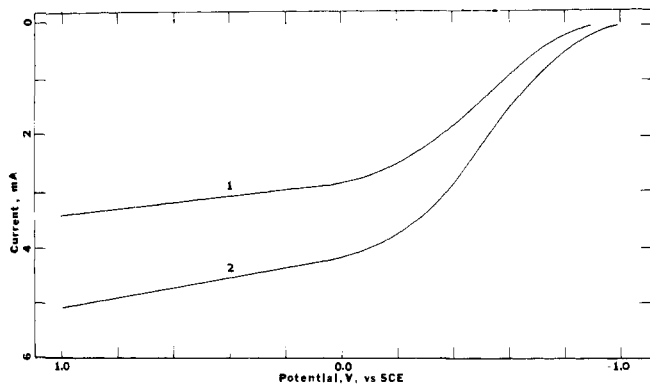


Figure 2. Current-potential curve for single-crystal  $\text{TiO}_2$  illuminated with a 450 W Xenon lamp: (1) in 0.1 M NaOH; (2) in 0.1 M NaOH and 1 M NaCN showing current doubling.

limiting anodic photocurrents in the presence and absence of the compounds (see Figure 2) assuming that the total current for substance oxidation is twice this difference current. It is possible that HQ and PAP, which undergo net 2e oxidations, also participate in a current doubling process, especially since current doubling has been invoked for the reduction of benzoquinone at GaP.<sup>37</sup> However, no increases of saturation photocurrent were observed for HQ and PAP above the level of the background solution and a noncurrent doubling process for these substances at  $\text{TiO}_2$  seems more likely. No increase in saturation photocurrent was observed when  $\text{S}^{2-}$  was added to the solution and the current efficiency for  $\text{S}^{2-}$  oxidation was assigned the value zero. In every case where significant participation of solution species other than water occurred, there was an obvious change in the  $i$ - $E$  curve compared to that found in the absence of oxidizable compounds. The  $i$ - $E$  curves were nearly identical with and without  $\text{S}^{2-}$ , which supports the conclusion that  $\text{S}^{2-}$  is not oxidized at an illuminated  $\text{TiO}_2$  electrode. The photoassisted oxidation currents for ethyl formate increased with time. The current efficiency values in Table 1 were the initial ones observed; the current efficiency eventually reached values as high as 0.5 to 0.6.

Fujishima and Honda<sup>38</sup> previously determined the current efficiency for  $\text{I}^-$  oxidation at a single crystal  $\text{TiO}_2$  electrode by measuring the pH change of the solution as the reaction progressed. Their measured current efficiency was 0.85 for both 0.01 and 0.1 M  $\text{I}^-$  concentrations. The latter result is in excellent agreement with ours while the former is somewhat higher. These authors<sup>39</sup> also made some measurements with bromide ion at a platinum ring  $\text{TiO}_2$  disk electrode. Using the ring disk parameters furnished, one can calculate corresponding current efficiencies<sup>40</sup> for 0.01, 0.1, and 1 M  $\text{Br}^-$  of about 0.3, 0.5, and 0.5. Shub et al.<sup>41</sup> reported that the current efficiency for the oxidation of chloride in 0.01 N HCl at  $\text{TiO}_2$  was 1.0. This value does not agree with our results nor does it follow the trend observed in this work and by others at different semiconductor electrodes for the current efficiencies of  $\text{I}^-$  through  $\text{Cl}^-$ . The current efficiencies for ethanol and several other alcohols in acidic solutions have been recently reported.<sup>42</sup>

In general the solution pH was adjusted in these measurements to give the slowest rates of direct reaction between oxygen and the added compound. However, for cases where the efficiency was determined at different pH's (e.g., with  $\text{I}^-$ ) there was no pronounced pH dependence. We also did not observe any significant difference in current efficiencies between single crystal and polycrystalline materials. However, there was an effect of supporting electrolyte composition. For example, the current efficiency for  $\text{I}^-$  oxidation decreased from 0.6 to 0.3 when a phosphate electrolyte was substituted for a sulfate one at a given pH. The current efficiencies in Table 1

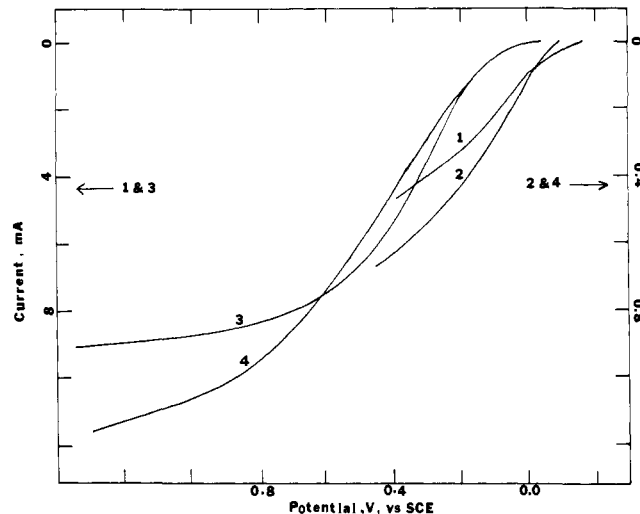
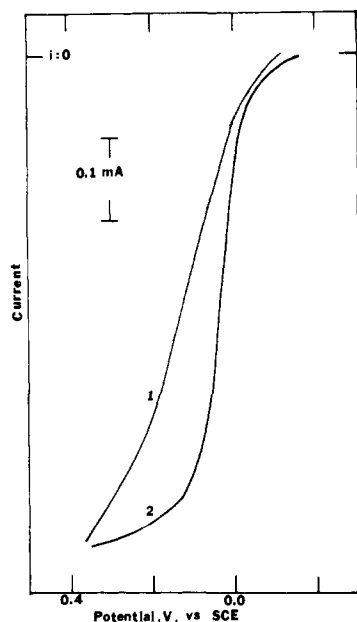


Figure 3. Current-potential curve for illuminated polycrystalline  $\text{TiO}_2$  in the presence and absence of *p*-aminophenol (PAP): (1) 30 mM PAP in 0.2 M  $\text{H}_2\text{SO}_4$  at full lamp intensity; (2) 30 mM PAP in 0.2 M  $\text{H}_2\text{SO}_4$  with neutral density filters; (3) 0.2 M  $\text{H}_2\text{SO}_4$  at full lamp intensity; (4) 0.2 M  $\text{H}_2\text{SO}_4$  with same filters as (2).

are not functions of the potential of the  $\text{TiO}_2$  electrode, suggesting that the reactivity of a hole for a compound is potentially independent. For example, HQ is oxidized with a current efficiency of 0.8 at both 0.2 and 1.2 V vs. SCE. All of the compounds were oxidized at the illuminated  $\text{TiO}_2$  electrode at potentials negative of those for their oxidation at platinum and negative of their reversible potentials (i.e., the oxidation at  $\text{TiO}_2$  occurred with a "negative overpotential"). The onsets of the oxidations were always slightly positive of  $V_{fb}$ .

**Current-Potential Curves.** Photocurrent-potential curves were determined for all of the substances in Table 1, with the exception of the anilines where electrodes filming occurred; typical results are given in Figures 3-5. The limiting currents in the presence of compound were often less than in their absence because of filtering of the incident UV radiation by the products. In every case where a current efficiency above 0.1 was found for the oxidation of the compound, the onset of the photocurrent occurred at a less positive potential than in the compound's absence. The magnitude of the potential shift was a function of pH, illumination intensity, nature of the electrode (polycrystalline or single crystal), and, for the polycrystalline material, the length of time the electrode was used as a photoanode. The onset of the photocurrent for newly prepared polycrystalline and single crystal electrodes activated in the same fashion under vacuum was the same.<sup>4</sup> Generally with time the onset of the photocurrent for the polycrystalline electrodes shifted to more positive potentials, especially in the acidic solutions, compared to the single crystal electrode. A decrease in the illumination intensity usually resulted in a decrease in the difference between the potentials for the onset of current when the compound was present and absent (Figure 3). Increasing the pH had a similar effect. We also often noticed a change in the steepness of the rising portion of the current-potential curve (Figure 4). Fujishima et al.<sup>43</sup> observed a similar change in curve shape. In all cases, except with  $\text{Ce}^{3+}$ , the open circuit potential of the  $\text{TiO}_2$  electrode when illuminated was nearly the same as that for the onset of the photocurrent. The open circuit potential with  $\text{Ce}^{3+}$  was about 0.1 V positive of the onset of the photocurrent. Photopotential effects have been discussed elsewhere.<sup>19,44,45</sup> The most negative potential the  $\text{TiO}_2$  electrode can have under these conditions is  $V_{fb}$ . The onset of the photocurrent has been previously associated with  $V_{fb}$  as determined by capacitance measurements (Shottky-Mott plots).<sup>46</sup> This in fact should be true in the ab-



**Figure 4.** Current-potential curve for illuminated single crystal  $\text{TiO}_2$  in the presence and absence of PAP. Output of 450 W Xenon lamp attenuated with neutral density filters: (1) absence of PAP, 0.2 M  $\text{H}_2\text{SO}_4$ ; (2) presence of 30 mM PAP in 0.2 M  $\text{H}_2\text{SO}_4$ .

**Table II.** Open Circuit Potential of the Illuminated  $\text{TiO}_2$  Electrode in the Presence and Absence of Various Compounds<sup>a</sup>

Compd	Potential (V vs. SCE)	
	Full lamp int.	$\frac{1}{10}$ lamp int.
0.2 M $\text{Na}_2\text{SO}_4$ (pH = 5.1) + 0.1 M NaI	-0.48	+0.46
0.2 M $\text{H}_2\text{SO}_4$ + 0.1 M NaI	-0.18	-0.18
0.2 M $\text{H}_2\text{SO}_4^b$ + 0.1 M NaI <sup>b</sup>	-0.34	-0.32
0.2 M $\text{H}_2\text{SO}_4^c$ + 0.1 M NaI	-0.16	
	-0.34	
0.2 M $\text{H}_2\text{SO}_4$ + 0.1 M NaBr	-0.06	
	-0.24	
0.2 M $\text{H}_2\text{SO}_4$ + 0.1 M NaCl	-0.18	-0.18
	-0.26	-0.28
0.2 M $\text{H}_2\text{SO}_4$ + 0.03 M HQ	-0.18	-0.18
	-0.23	-0.18
0.2 M $\text{H}_2\text{SO}_4$ + 0.03 M PAP	-0.24	-0.18
	-0.18	-0.18
0.2 M $\text{H}_2\text{SO}_4^b$ + 0.03 M PAP <sup>b</sup>	-0.18	-0.10
	-0.16	
0.2 M $\text{H}_2\text{SO}_4^c$ + 10 mM HQ	-0.19	
	-0.02	
0.2 M $\text{H}_2\text{SO}_4^c$ + 10 mM $\text{Fe}(\text{CN})_6^{4-}$	-0.15	
	-0.06	
0.2 M $\text{H}_2\text{SO}_4^c$ + 10 mM $\text{Fe}^{2+}$ + 30 mM $\text{Fe}^{2+}$	-0.12	
	-0.04	
	-0.17	
	-0.17	
0.2 M $\text{H}_2\text{SO}_4^c$ + 30 mM $\text{Ce}^{3+}$	-0.03	
	-0.01	

<sup>a</sup> Electrode was polycrystalline unless noted. <sup>b</sup> Single crystal. <sup>c</sup> These experiments were done at different times than the others and show the dependence of the open circuit potential on time.

sense of surface or space charge recombination phenomena. The open circuit potentials are tabulated in Table II. These potentials also depended on the illumination intensity, solution

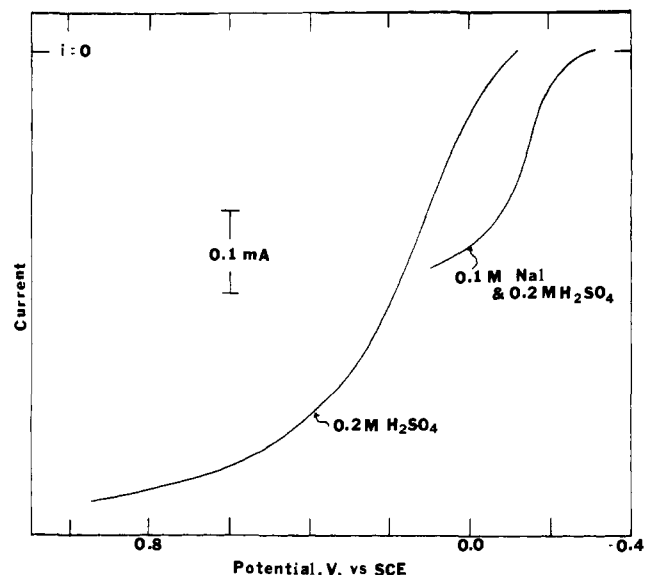


**Figure 5.** Current-potential curves for illuminated single-crystal  $\text{TiO}_2$  in the presence and absence of NaI. Light intensity of 450 W lamp attenuated with neutral density filters.

pH, and nature of the electrode. For similar type compounds there was a rough correlation between the shift in the open circuit potential of the illuminated  $\text{TiO}_2$  and the current efficiency of the compound added. The significance of these results is discussed below.

**Photooxidation Products.** The oxidation products at the  $\text{TiO}_2$  electrode were generally the same as those formed by oxidation at a platinum electrode. Thus the halides were oxidized to the free halogens, as demonstrated by their volatility and a starch-iodide test. Other products were identified by their electrochemical behavior at either a platinum or  $\text{TiO}_2$  electrode. For example, a convenient method of identifying a primary product of oxidation which was not stable over a longer time period involved using a reversal technique (Figure 6). The reduction waves of various species which are reduced above or near the conduction band of  $\text{TiO}_2$ , e.g., *p*-benzoquinone (BQ), occur at characteristic potentials. Thus by holding the potential of the illuminated electrode at a potential where photooxidation of substrate (e.g., HQ) occurs and then sweeping linearly toward negative potentials, the reduction wave of product can be observed. Similarly, for PAP a first reduction wave characteristic of the quinone imine appears at more positive potentials than that for BQ reduction, when a rapid sweep is made to positive potentials in the light. If the electrode potential is maintained for several seconds at +0.2 V under illumination a second reduction wave appears on the reverse scan at the same potential as BQ reduction, suggesting hydrolysis of the quinone imine to BQ and paralleling the behavior observed at platinum electrodes.<sup>47</sup> At longer times the oxidation products of both HQ and PAP undergo further, presumably photocatalyzed, reactions. The nature of these reactions and the ultimate products were not investigated further, but 1,4-addition<sup>48</sup> and cycloaddition<sup>49</sup> reactions are known for these types of compounds. Product analysis was not carried out for the species undergoing current doubling ( $\text{CN}^-$ , ethanol, ethyl formate) or for aniline and *N,N*-dimethylaniline.

**Photoelectrosynthesis.** Of particular interest is the application of photoassisted electrolysis at a semiconductor as a means of utilizing radiation (e.g., solar energy) for carrying out a redox process. This may be of interest in the chemical storage of solar energy or in the synthesis of a material of interest. Several possible processes are possible: (1) direct oxidation (e.g., HQ to BQ), (2) indirect oxidation (e.g.,  $\text{Ce}^{3+}$  to

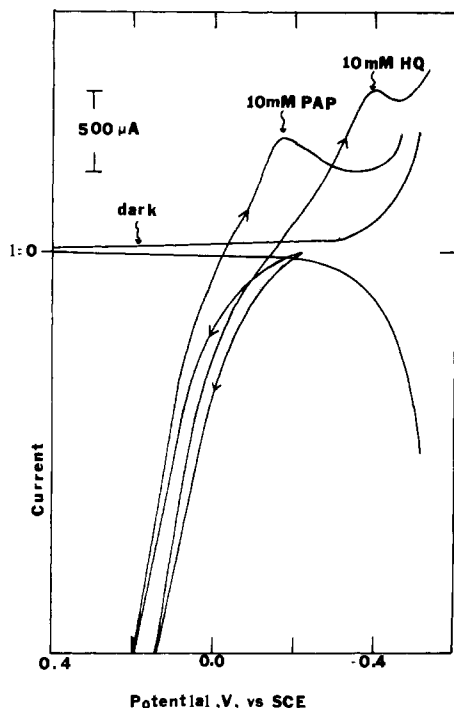


**Figure 6.** Photoassisted oxidation of PAP and hydroquinone (HQ) in 0.2 M  $\text{H}_2\text{SO}_4$  at polycrystalline  $\text{TiO}_2$  and reduction of the oxidation product. Sweep rate = 0.2 V/s.

$\text{Ce}^{4+}$ , followed by reaction of  $\text{Ce}^{4+}$  with the substrate regenerating  $\text{Ce}^{3+}$ , and (3) addition reactions of photogenerated product (e.g., formation of bromine or iodine which can then add to a substrate). Redox processes at semiconductors have the advantage over homogeneous photolytic processes of efficient separation of electrons and holes with little recombination. They suffer with respect to electrolytic processes at metal electrodes, since the potential at the electrode-solution interface cannot be varied and selectivity between possible oxidations will follow the relative current efficiencies of the different processes. For example, a process of interest would be the photooxidation of  $\text{I}^-$  to  $\text{I}_2$  followed by its reaction with aniline to form *p*-iodoaniline.<sup>50</sup> Unfortunately, at concentrations of  $\text{I}^-$  high enough to suppress direct aniline oxidation, the reaction between  $\text{I}_2$  and aniline was extremely slow. At lower  $\text{I}^-$  concentrations not only was a significant portion of the aniline oxidized directly but the volatility of  $\text{I}_2$  was too high for significant reaction to occur before most of the  $\text{I}_2$  disappeared from solution. We were more successful in attempts to react aniline with photogenerated bromine to form the tribromoaniline product.<sup>35</sup> By working at low concentrations of aniline and high concentrations of  $\text{Br}^-$  and using high current densities at the  $\text{TiO}_2$  so that the oxidation of aniline was mass transfer controlled but that of bromide was not, we were able to isolate tribromoaniline from the product solution. The spectral evidence is shown in Figure 7. Spectrum 2 is the product of the reaction of aniline with excess  $\text{Br}_2$  and should correspond to tribromoaniline.<sup>50</sup> We prefer this spectrum to any other for tribromoaniline, since it reflects any impurities that may have been present in the aniline reactant. The result of the photooxidation of  $\text{Br}^-$  at  $\text{TiO}_2$  in the presence of aniline is shown as spectrum 3. The differences between spectra 2 and 3 may be partly due to a small amount of unreacted aniline in the case of 3.

**Solar Cell Studies.** While the previously described experiments involved the  $\text{TiO}_2$  electrode maintained at a given potential by a potentiostat, it is also possible to carry out the photoassisted oxidations in a cell with no connections to an external power supply. We recently described such a cell

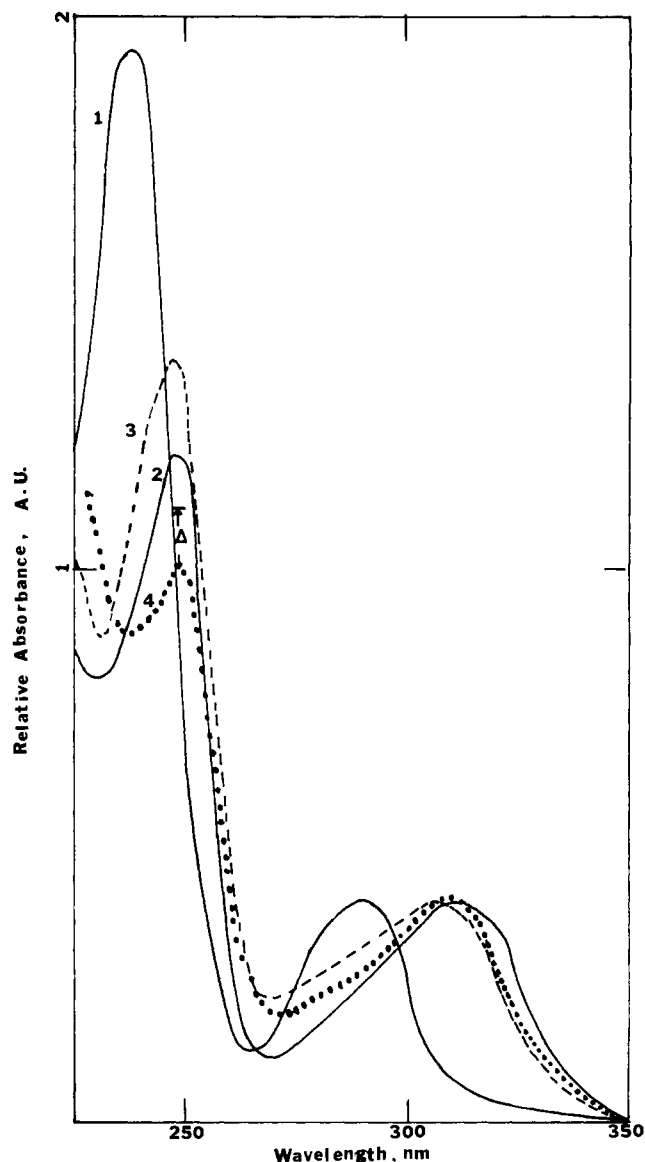


**Figure 7.** Spectrum of: (1) aniline, 0.1 mM, extracted from 0.2 M  $\text{Na}_2\text{SO}_4$  with ether; (2) 0.1 mM aniline after reaction with excess  $\text{Br}_2$  (liquid), extracted from 0.2 M  $\text{Na}_2\text{SO}_4$  with ether after removing excess  $\text{Br}_2$  by degassing with  $\text{N}_2$ ; (3) 0.1 mM aniline and 0.1 M  $\text{NaBr}$  in 0.2 M  $\text{Na}_2\text{SO}_4$  following controlled potential photoassisted oxidation at  $\text{TiO}_2$  (2.2 C of electricity, passed), extracted with ether after degassing with  $\text{N}_2$ ; (4) 0.01 mM aniline and 1 M  $\text{NaBr}$  in 0.2 M  $\text{Na}_2\text{SO}_4$  following 50 s of photoassisted oxidation at  $\text{TiO}_2$  on platinum in solar cell with platinum fuel cell cathode and extraction with ether after degassing with  $\text{N}_2$ . The relative uncertainty of the absorbance is  $\Delta$ .

employing a polycrystalline  $\text{TiO}_2$  photoanode and a fuel-cell electrode cathode for the production of electrical energy under illumination.<sup>11</sup> In that study oxygen was generated at the  $\text{TiO}_2$  and reduced at the cathode. If an oxidizable substance is added to the cell, the net reaction consists of photooxidation of the substrate and reduction of oxygen. Because higher currents can be sustained at the cathode compared to the  $\text{TiO}_2$  anode (i.e., the cathode is less polarizable than the anode), the potential of the  $\text{TiO}_2$  electrode during illumination is maintained at essentially the dark potential of the oxygen cathode vs. the SCE. Thus, for a solution that is 0.2 M  $\text{Na}_2\text{SO}_4$  and 2 mM  $\text{H}_2\text{SO}_4$  the cathode potential is 0.5 to 0.6 V vs. SCE. This cell can be used to oxidize the compounds in Table I. The construction of the cell is such that the compound is confined to a region between the optical window and  $\text{TiO}_2$  electrode (in a total volume of about 10 mL) and did not contact the cathode. Compounds with redox potentials negative of the cathode

potential are thermodynamically capable of reacting directly with oxygen and could react in this solar cell arrangement even in the absence of light. For these the dark currents were about 0.2 to 0.3 the magnitude of the photocurrents. The existence of dark currents suggests that the TiO<sub>2</sub> film is permeable and the solution can contact the platinum substrate. In all cases, however, the extent of conversion to product was greater for the illuminated electrode. When the compounds had redox potentials positive of the oxygen cathode potential, the dark current was very small. The current-time behavior for the TiO<sub>2</sub>/Pt(O<sub>2</sub>) cathode cell containing 1 M NaBr, 0.2 M Na<sub>2</sub>SO<sub>4</sub>, and 2 mM H<sub>2</sub>SO<sub>4</sub> is shown in Figure 8. The gradual decay in current during the light-on pulses is due to filtering of the light by the photogenerated Br<sub>2</sub>. When the light was turned off, a small back-current was observed, probably caused by reduction of Br<sub>2</sub> at exposed platinum on the TiO<sub>2</sub> coated electrode and oxidation of water or a residual reductant at the counter electrode. The oxidation of bromide in the presence of aniline could also be accomplished. However, because the area of the photoanode was much larger than in the potentiostatic experiment (30 cm<sup>2</sup> vs. 1 cm<sup>2</sup>), the current densities obtainable at the available light intensity were smaller and lower aniline concentrations and short oxidation times were required to produce the tribromoaniline (see spectrum 4 of Figure 7). At higher aniline concentrations the 248-nm peak decreased relative to the long wavelength absorbance and eventually disappeared altogether; this suggests substantial direct oxidation of aniline before it reacts with Br<sub>2</sub>.

A bright platinum foil with the same projected area as the fuel cell electrode could also serve as the oxygen counter electrode. Although the open circuit potential of this foil was nearly the same as that of the fuel cell oxygen electrode, when it was connected to the illuminated TiO<sub>2</sub>, the potential vs. an SCE shifted to more negative values. With moderate O<sub>2</sub> bubbling the potential assumed for the illuminated TiO<sub>2</sub> and platinum electrodes was about +0.05 V vs. SCE for 0.2 M H<sub>2</sub>SO<sub>4</sub> and the current was about 1 mA. Using the solar cell and this electrode combination, we were able to oxidize the compounds in Table I even though the measured potentials of both the TiO<sub>2</sub> and platinum electrodes were negative of the potentials for their oxidations at platinum.

We also found that the TiO<sub>2</sub>-coated platinum electrode alone could serve the function of both anode and cathode. Illuminating an air-saturated 1 M NaBr solution in contact with only this electrode resulted in bromine formation. When the experiment was repeated with a platinum foil replacing the TiO<sub>2</sub> electrode, no bromine was formed. Thus the TiO<sub>2</sub>-coated electrode behaves as a short circuited cell with oxygen apparently reduced at bare platinum sites and bromide oxidized at the TiO<sub>2</sub> sites. Useful particulate heterogeneous photocatalytic systems can be devised based on the measured properties of the electrodes. Indeed we have recently described the photocatalytic oxidation of CN<sup>-</sup> at different TiO<sub>2</sub> powder suspensions.<sup>58</sup>

## Discussion

A significant aspect of this work is the demonstration that a rather large variety of compounds can undergo photoassisted oxidation at TiO<sub>2</sub> sometimes with very high current efficiencies. Previous studies at other semiconductors<sup>23,24,26,36,51</sup> have demonstrated the oxidation of solution species but these studies were generally directed at determining the role of holes in semiconductor processes rather than illustrating any synthetic applications. In the present study an overall conversion of as much as 20% of a compound to its product (in a solution volume of about 30 mL) was accomplished. The major factor that prevented higher conversions was the filtering of the incident light by the product of the electrode reaction and the relatively

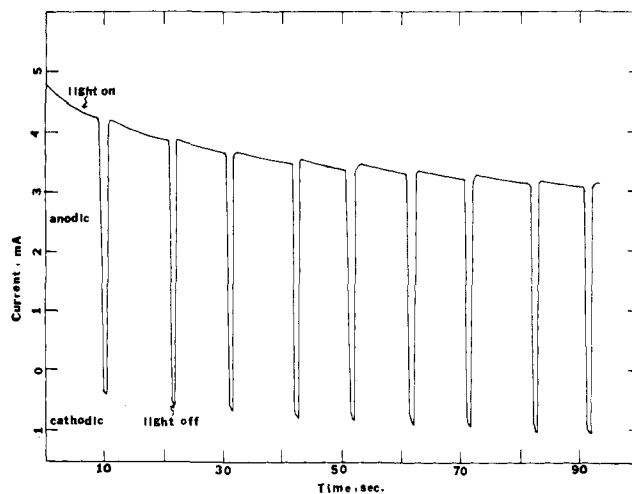


Figure 8. Current-time behavior of 1 M NaBr at TiO<sub>2</sub> on platinum with fuel cell cathode (no external power supply) with and without light from 450 W Xenon lamp. Current measured through 1 Ω resistor connected between anode and cathode.

small size of the electrode. The system could clearly be scaled up, especially with a thin reaction layer and flow cell arrangement, to carry out relatively complete bulk photoelectrolysis. Because the photoassisted oxidations occur at less negative potentials at n-type materials compared to metal electrodes, every 0.1-V shift in the potential is equivalent to a saving of as much as 2 kcal/mol of electrical energy. This could amount to 32 kcal/mol for Br<sup>-</sup> and Ce<sup>3+</sup> oxidation at a current efficiency of 1; at lower efficiencies the energy savings is decreased accordingly.

The products of the oxidations at TiO<sub>2</sub> corresponded to the most easily formed species at a platinum electrode. Some of these compounds can be further oxidized at platinum at more positive potentials. There was no evidence of further oxidation at TiO<sub>2</sub> but this may be because the conversions were incomplete and there was not enough product at the TiO<sub>2</sub> surface to compete for holes with the unreacted starting material. Further oxidation of product has been seen at CdS.<sup>36</sup> Differences in absorbability between the reactant and product could also be important, if absorption is a prerequisite for the photooxidation.

The ability of so many compounds to compete successfully with water for photogenerated holes is interesting, especially since the water concentration is about 55 M. Thus the reactivity of some of these compounds with photogenerated holes approaches 10<sup>4</sup> times the reactivity of water. There are several possible effects which can lead to this difference in reactivity and which are important as well in the prevention of decomposition of small band-gap semiconductors (e.g., CdS, GaAs) by the addition of solution species which can be electrolyzed competitively. According to the model of Gerischer and others<sup>19</sup> the rate of charge transfer across the interface depends upon the relative distribution of states in the semiconductor and solution, i.e.,

$$i_{\text{ox}} \propto C_R \int_{-\infty}^0 \kappa(E) D_+(E) W_R(E) dE \quad (2)$$

where  $i_{\text{ox}}$  is the anodic current,  $C_R$  is the concentration of reduced species in solution,  $D_+(E)$  is the density of unoccupied states (in this case, photogenerated holes) in the semiconductor of energy,  $E$ , and  $W_R(E)$  is the distribution function of the reduced state in solution. Assuming that charge transfer occurs only at discrete energies, i.e., at the valence band edge or at a surface state, this expression can be simplified to

$$i_{\text{ox}} \propto C_R [\kappa(E_{\text{ss}}) D_+(E_{\text{ss}}) W_R(E_{\text{ss}}) + \kappa(E_{\text{VB}}) D_+(E_{\text{VB}}) W_R(E_{\text{VB}})] \quad (3)$$

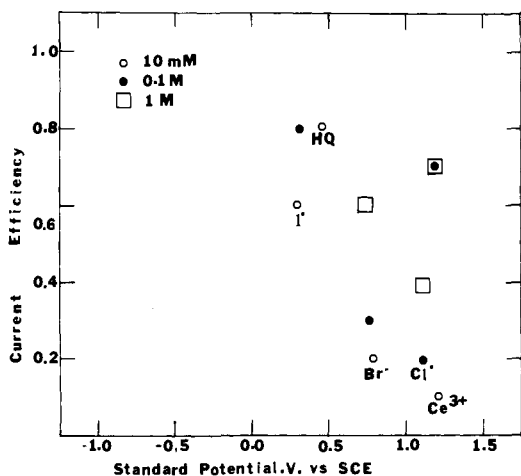


Figure 9. Current efficiency as a function of standard redox potential for a number of the compounds of this investigation.

where  $E_{ss}$  and  $E_{VB}$  represent the energy of any surface states (only one such level is assumed for simplicity) and the energy of the valence band edge, respectively. Except for  $C_R$  the terms on the rhs of the above equation are constant, so that

$$i_{ox} \propto C_R \kappa(E_{ss}, E_{VB}) \quad (4)$$

The total current  $i_T$ , representing hole transfer to different species, is the sum of such expressions. In the present case there are two such terms,

$$i_T = C_R \kappa(E_{ss}, E_{VB}) + C_{H_2O} \kappa'(E_{ss}, E_{VB}) \quad (5)$$

where  $C_{H_2O}$  is the concentration of water (55 M). Since the total current cannot exceed the flux of photogenerated holes,  $i_T$  is constant and changes in  $C_R$  serve to alter the fraction of the current that goes to the oxidation of R and  $H_2O$ . We assume that recombination effects are minor and the overall quantum efficiency is high and independent of  $C_R$ . One can easily show that the hole current participating in the oxidation of R,  $i_{ox}(R)$ , and the current efficiency in terms of the total current,  $i_T$ , is

$$\begin{aligned} \text{curr. eff.} &= \frac{i_{ox}(R)}{i_T} \\ &= \left[ \frac{\kappa(E_{ss}, E_{VB})}{\kappa(E_{ss}, E_{VB}) + C_{H_2O} [\kappa'(E_{ss}, E_{VB}) / C_R]} \right] \quad (6) \end{aligned}$$

This equation predicts an S-shaped current efficiency vs. concentration curve with  $i_{ox}$  approaching  $i_T$  as  $C_R$  approaches large values.

The ability of solution compounds to compete with water for holes is dependent on the relative values  $\kappa(E_{ss}, E_{VB})$  and  $\kappa'(E_{ss}, E_{VB})$ . As formulated above these rate constants are primarily influenced by the degree of overlap of solution levels with hole-containing semiconductor levels. However, other factors such as adsorption of solution species onto the semiconductor surface may affect these rate constants either by creating new surface states or by altering the energy of existing states or levels. In the absence of adsorption the overlap model predicts increasing overlap of solution levels with the top of the valence band as the redox potential becomes more positive. The current efficiency for the photoassisted oxidation is then predicted to increase with couples of progressively more positive  $E^\circ$  values, if holes are generated only in the valence band. This is opposite of the trend in Table I and Figure 9, as well as results of others on different materials.<sup>27</sup> Thus the behavior cannot be explained by the sample model of Gerischer where charge transfer is assumed to occur only through the valence band. An attractive explanation for the observed results is the

participation of energy states in the band gap. The possible existence of such an intermediate level at  $TiO_2$  has been suggested by previous studies of the behavior of  $TiO_2$  in acetonitrile (MeCN) solutions.<sup>20</sup> If the energy of the proposed level remains the same in water as in MeCN (i.e., about 1.2 eV below the conduction band) it is possible to explain the present results on the basis of overlap with this level. For very positive couples with large reorganizational energies for charge transfer, overlap of filled solution levels with valence band becomes possible and a reversal in the decreasing trend in current efficiencies with increasingly positive redox potentials may occur, as is seen at some concentrations of  $Ce^{3+}$ .

It is also possible that adsorption of solution species plays an important role in the current efficiency. A regular variation in current efficiency within a series of similar compounds, such as  $I^-$ ,  $Br^-$ ,  $Cl^-$ , might be attributed to adsorption by analogy to metal electrodes.<sup>52</sup> The same trend for the halides is also seen on ZnO and CdSe.<sup>24,26</sup> The observed effect of phosphate on the current efficiency of  $I^-$  is best understood by competitive adsorption, with phosphate displacing  $I^-$ . Strong adsorption of  $Fe^{2+}$  and  $Ce^{3+}$  on  $SnO_2$  is known<sup>53</sup> and a similar adsorption mechanism seems possible on  $TiO_2$ . The differences in current efficiencies between different semiconductors may in part be explained by differences in adsorption. The current efficiency for  $CN^-$  oxidation at ZnO is 0.7<sup>54</sup> compared to 0.4 at  $TiO_2$  in spite of the similar band structure of  $TiO_2$  and ZnO,<sup>55</sup> although differences in the distributions of intermediate energy levels may also explain these differences.

Changes in solution pH result in large changes in the surface structure of  $TiO_2$ <sup>46</sup> by the introduction of charged groups on the surface. One would expect a dependence of current efficiency on pH, if adsorption of the reactant takes place. Our results showed no such dependency. However, our pH studies were limited by a desire to obtain the maximum compound stability; a study of the dependence of current efficiency on pH should be of interest.

The oxidation of a compound in a solar cell as described here without any external electrical energy is analogous to photosynthesis. The cell in principle carries out a useful chemical transformation and consumes only inexpensive and readily available materials. We are not aware of any other useful transformation, other than the conversion of water to  $H_2$  and  $O_2$ , that has been demonstrated. In the latter case a pH differential was necessary for the reaction to proceed at a reasonable rate at  $TiO_2$ .<sup>3</sup> In the present examples both electrodes were surrounded by the same electrolyte.

For the conversion of solar to electrical energy, this cell could be modified by using a redox couple with a potential below  $V_{fb}$  of the semiconductor.<sup>17</sup> The more positive  $V_{fb}$  of the couple is, the more efficient the cell will be under illumination, since the effect of light is to change the potential in the direction of the flatband potential. In operation, one component of the redox couple will be oxidized at the  $TiO_2$  while reduction of the other component occurs at the cathode.<sup>17</sup> If the current efficiency at the semiconductor is less than 1, the overall efficiency of the cell will decrease, since eventually some electrical energy will have to be used to restore the cell to its original state.

The negative shift in the potential for the onset of the photocurrent and the change in the shape of the current-potential curve when certain compounds are added is of interest. Both occurrences bring about an increase in efficiency for carrying out a particular process, since less potential need be applied to the cell to obtain the same current. If the onset of the photocurrent corresponds to the flatband potential, this is the first time such a shift has been seen for  $TiO_2$ . The observed shift in the potential in most cases is too small to allow unambiguous assignment of a change in  $V_{fb}$  from capacitance measurements. The specific adsorption of negatively charged compounds can cause a change in  $V_{fb}$  by introduction of negative charge onto



the TiO<sub>2</sub> surface. However, a similar explanation will not hold for the positively charged ions.

An alternate explanation especially for the change in the shape of the current-potential curves involves the role of recombination phenomena. The shape of the current-potential curves and the onset of a photocurrent is determined by a number of factors.<sup>19,44,56</sup> Among these are the thickness and electric field in the space charge region, the rate of recombination in the space charge region and just outside of it, surface recombination, and the back electron transfer reaction of the oxidation product. In the absence of such recombination phenomena, the shape of the current-potential curve is determined by the efficiency with which the photogenerated electron-hole pairs are separated. The efficiency of the separation increases as the polarization of the semiconductor is increased positive of the flatband potential, because both the field and thickness of the space charge region become larger. A limiting current is eventually reached when the thickness of the space charge region approaches the depth of penetration of the light. Recombination phenomena mediated by recombination centers located energetically within the semiconductor band gap are potential dependent and have the greatest effect over a rather limited potential range where the levels are only partially occupied. The effect of a single energy level for fast recombination can be to shift the current-potential curve along the potential axis as seen in the case of adsorbed metal atoms.<sup>57</sup> More than one energy level may result in a more drawn out curve. The back reaction can be viewed as a special case of surface recombination. That recombination events are important for TiO<sub>2</sub> can be seen in Figure 4. If no surface recombination occurred in TiO<sub>2</sub> and the photocurrent was only controlled by the supply of holes to the surface, there should be no difference in the current-potential curve when PAP is added. Instead, the curve rises more sharply indicating that surface recombination has been suppressed. Illumination intensity can also have an effect, if an incremental increase in electron-hole generation is not matched by a similar increase in recombination (Figure 6).

**Acknowledgment.** The support of this research by the National Science Foundation (MPS74-23210) and the Welch Foundation is gratefully acknowledged.

## References and Notes

- (1) A. Fujishima and K. Honda, *Nature (London)*, **238**, 37 (1972).
- (2) H. Yoneyama, H. Sakamoto, and H. Tamura, *Electrochim. Acta*, **20**, 341 (1975).
- (3) A. Fujishima, K. Kohayakawa, and K. Honda, *Bull. Chem. Soc. Jpn.*, **48**, 1041 (1975).
- (4) K. L. Hardee and A. J. Bard, *J. Electrochem. Soc.*, **122**, 739 (1975).
- (5) J. Keeney, D. H. Weinstein, and G. M. Haas, *Nature (London)*, **253**, 719 (1975).
- (6) A. J. Nozik, *Nature (London)*, **257**, 383 (1975).
- (7) M. S. Wrighton, D. S. Ginley, P. T. Wolczanski, A. B. Ellis, D. J. Morse, and A. Linz, *Proc. Natl. Acad. Sci. U.S.A.*, **72**, 1518 (1975).
- (8) A. Fujishima, K. Kohayakawa, and K. Honda, *J. Electrochem. Soc.*, **122**, 1487 (1975).
- (9) M. S. Wrighton, D. T. Morse, A. B. Ellis, D. S. Ginley, and H. B. Abrahamson, *J. Am. Chem. Soc.*, **98**, 44 (1976).
- (10) K. L. Hardee and A. J. Bard, *J. Electrochem. Soc.*, **123**, 1024 (1976).
- (11) D. Laser and A. J. Bard, *J. Electrochem. Soc.*, **123**, 1027 (1976).
- (12) G. Hodes, J. Monassen, and D. Cahen, *Nature (London)*, **261**, 403 (1976).
- (13) A. B. Ellis, S. W. Kaiser, and M. S. Wrighton, *J. Am. Chem. Soc.*, **98**, 6418 (1976).
- (14) A. B. Ellis, S. W. Kaiser, M. S. Wrighton, *J. Am. Chem. Soc.*, **98**, 1635 (1976).
- (15) B. Miller and A. Heller, *Nature (London)*, **262**, 680 (1976).
- (16) (a) A. Rathwarf and K. W. Boer, *Prog. Solid State Chem.*, **10**, 71 (1975); (b) M. D. Archer, *J. Appl. Electrochem.*, **5**, 17 (1975).
- (17) H. Gerischer, *J. Electroanal. Chem.*, **58**, 263 (1975).
- (18) D. Wong and B. DeBartolo, *J. Photochem.*, **4**, 249 (1975).
- (19) (a) H. Gerischer, "Physical Chemistry: An Advanced Treatise", Vol. 9A, H. Eyring, D. Henderson, and W. Jost, Ed., Academic Press, New York, N.Y., 1970; (b) H. Gerischer, *Adv. Electrochem. Electrochem. Eng.*, **1**, 139 (1961).
- (20) S. N. Frank and A. J. Bard, *J. Am. Chem. Soc.*, **97**, 7427 (1975).
- (21) D. L. Laser and A. J. Bard, *J. Phys. Chem.*, **80**, 459 (1976).
- (22) B. Pettinger, H. R. Schoppel, and H. Gerischer, *Ber. Bunsenges. Phys. Chem.*, **78**, 1024 (1974).
- (23) K. Hauffe and J. Range, *Ber. Bunsenges. Phys. Chem.*, **71**, 690 (1967).
- (24) W. P. Gomes, T. Freund, and S. R. Morrison, *J. Electrochem. Soc.*, **115**, 818 (1968).
- (25) H. Gerischer and W. Mendt, *Electrochim. Acta*, **13**, 132 (1968).
- (26) R. A. L. Vanden Bergh, W. P. Gomes, and F. Cardon, *Z. Phys. Chem. (Frankfurt am Main)*, **92**, 91 (1974).
- (27) T. Inoue, K. Kohayakawa, T. Watanabe, A. Fujishima, K. Honda, *J. Electrochem. Soc.*, submitted.
- (28) S. A. Dunn, *J. Am. Chem. Soc.*, **76**, 619 (1954).
- (29) T. Watanabe, A. Fujishima, and K. Honda, *Chem. Lett.*, 897 (1974).
- (30) W. M. Latimer, "Oxidation Potentials", 2nd ed, Prentice-Hall, Englewood Cliffs, N.J., 1952.
- (31) P. J. Boddy, *J. Electrochem. Soc.*, **115**, 199 (1968).
- (32) F. Mollers, H. J. Tolle, and R. Memming, *J. Electrochem. Soc.*, **121**, 1160 (1974).
- (33) T. Ohnishi, Y. Nakato, and H. Tsubomura, *Ber. Bunsenges. Phys. Chem.*, **79**, 523 (1975).
- (34) H. A. Latinen, "Chemical Analysis", McGraw-Hill, New York, N.Y., 1960.
- (35) J. J. Lingane, "Electroanalytical Chemistry", 2nd ed, Interscience, New York, N.Y., 1958.
- (36) H. Gerischer and H. Rosler, *Chem. Ing. Tech.*, **42**, 176 (1970).
- (37) R. Memming and F. Mollers, *Ber. Bunsenges. Phys. Chem.*, **76**, 609 (1972).
- (38) A. Fujishima and K. Honda, *J. Chem. Soc. Jpn.*, **74**, 355 (1971).
- (39) A. Fujishima and K. Honda, *Seisan Kenkyu*, **22**, 478 (1970).
- (40) W. J. Albery and S. Bruckenstein, *Trans. Faraday Soc.*, **62**, 1920 (1966).
- (41) D. M. Shub, A. A. Remnev, and V. I. Veselovskii, *Elektrokhimiya*, **9**, 1043 (1973).
- (42) M. Miyake, H. Yoneyama, and H. Tamura, *Chem. Lett.*, 635 (1976).
- (43) A. Fujishima, K. Honda, and S. Kikuchi, *J. Chem. Soc. Jpn.*, **72**, 108 (1969).
- (44) H. Gerischer, *J. Electrochem. Soc.*, **113**, 1174 (1966).
- (45) V. A. Myamlin and Y. V. Pleskov, "Electrochemistry of Semiconductors", Plenum Press, New York, N.Y., 1967.
- (46) A. Fujishima, A. Sakamoto, and K. Honda, *Seisan Kenkyu*, **21**, 450 (1969).
- (47) (a) C. R. Christensen and F. C. Anson, *Anal. Chem.*, **36**, 495 (1964).
- (48) R. N. Adams, "Electrochemistry at Solid Electrodes", Marcel Dekker, New York, N.Y., 1969.
- (49) N. J. Bunce and M. Hadley, *Can. J. Chem.*, **53**, 3246 (1975).
- (50) V. Migrdechian, "Organic Synthesis", Vol. 2, Reinhold, New York, N.Y., 1957.
- (51) A. Fujishima, E. Sugiyama, and K. Honda, *Bull. Chem. Soc. Jpn.*, **44**, 304 (1971).
- (52) (a) R. Payne, *Trans. Faraday Soc.*, **64**, 1638 (1968); (b) J. Lawrence, R. Parsons, and R. Payne, *J. Electroanal. Chem.*, **16**, 193 (1968); (c) D. C. Grahame, *J. Am. Chem. Soc.*, **80**, 4201 (1958).
- (53) P. R. Moses, L. Wier, and R. W. Murray, *Anal. Chem.*, **47**, 882 (1975).
- (54) S. R. Morrison and T. Freund, *Electrochim. Acta*, **13**, 1343 (1968).
- (55) M. Gleria and R. Memming, *J. Electroanal. Chem.*, **65**, 163 (1973).
- (56) D. Laser and A. J. Bard, *J. Electrochem. Soc.*, **123**, 1837 (1976).
- (57) D. M. Kolb, M. Przasnyski, and H. Gerischer, *Z. Phys. Chem. (Frankfurt am Main)*, **93**, 1 (1974).
- (58) S. N. Frank and A. J. Bard, *J. Am. Chem. Soc.*, **99**, 303 (1977).